Interpretation of the temperature dependence of the luminescence intensity, lifetime, and decay profiles in porous Si

T. Suemoto and K. Tanaka
Institute for Solid State Physics, The University of Tokyo, Roppongi, Minato-ku, Tokyo 106, Japan

A. Nakajima
Fujitsu Laboratories Ltd., 10-1 Morinosato-Wakamiya, Atsugi-shi, Kanagawa-ken 243-01, Japan
(Received 7 July 1993; revised manuscript received 1 October 1993)

The temperature dependences of the luminescence intensity, lifetime, and decay profiles for porous Si are studied from 5 to 271 K. The radiative decay rates were determined from the tails of the decay curves and found to have an activation-type temperature dependence above 10 K. To describe the nonradiative process we propose a model in which we assume a tunneling and a thermally activated escape of the photoexcited carriers through barriers with a Gaussian distribution in height. The temperature dependence of intensity, lifetime, and nonexponential decay profiles are successfully interpreted in terms of this model.

INTRODUCTION

Since the discovery of intense visible luminescence in porous Si,[1] the mechanism of the luminescence has been a matter of controversy, and the luminescence properties have been studied extensively by means of both static and dynamic measurements. In spite of these efforts, the origin and the mechanism of the luminescence are not yet clear. Above all, understanding of the radiative and nonradiative processes in this system is particularly important, not only to clarify the luminescence mechanism, but also to improve the luminescence efficiency of the system for possible applications as light-emitting devices. The luminescence lifetime and decay profiles have been studied on various time scales by several authors; in the psec region by Matsumoto *et al.*[2] and in the nsec region by Gardelis *et al.*[3] and Miyoshi, Lee, and Aoygi.[4] In the μsec–msec region, the temperature dependence above room temperature (RT) was reported by Vial *et al.*[5] They interpreted the temperature and excitation-wavelength dependence of the lifetime in terms of luminescence quenching due to tunneling escape of carriers from the Si particles. On the other hand 't Hooft *et al.*[6] studied the temperature dependence of the lifetime down to 4.3 K and concluded that nonradiative processes are not a major decay channel and that the lifetime is essentially determined by radiative decay, which shows an activation-type temperature dependence. Recently, Calcott *et al.*[7] have shown that the temperature dependence of the lifetime of a long-lived component can be interpreted in terms of singlet-triplet exciton doublets localized in Si wires. Although these data cannot be compared directly because of possible differences in the samples and the large differences in the time scales, there are some common features. These features may be summarized as follows.

(i) The lifetime is longer at lower temperatures (in the μsec range reported by Vial *et al.*,[5] 't Hooft *et al.*,[6] and Calcott *et al.*[7]).

(ii) The lifetime is longer at longer wavelength under the same excitation wavelength (in the nsec range reported by Miyoshi, Lee, and Aoyagi,[4] in the psec range by Matsumoto *et al.*,[2] and in the μsec range by Vial *et al.*,[5] 't Hooft *et al.*,[6] and Calcott *et al.*[7]).

(iii) The luminescence intensity increases when the temperature is lowered from room temperature (in the nsec range reported by Gardelis *et al.*,[3] and in the μsec range by Vial *et al.*[5]).

(iv) The decay curve has a nonexponential shape (in the μsec range reported by Ookubo *et al.*[8] and Vial *et al.*,[5] in the psec range by Matsumoto *et al.*,[2] and in the nsec range by Matsumoto *et al.*,[2] Miyoshi, Lee, and Aoyagi[4] and Gardelis *et al.*[3])

As for (iii) and (iv), however, 't Hooft *et al.*[6] claim that the intensity is almost constant from RT to 4.3 K, and the decay curve is close to a single exponential. In addition, some of the authors note that the lifetime depends on the oxidation level of the samples.[5]

To the best knowledge of the authors, there has been no publication which can fully interpret the nonexponential decay profiles and their temperature dependences. In this paper, we investigate the decay behaviors of luminescence at various temperatures and propose a model which can describe these behaviors quantitatively and comprehensively between RT and liquid-He temperature.

EXPERIMENT

The porous Si samples we used were made from (100)-oriented *p*-type silicon substrates with a resistivity of 9–11 Ω cm. Al films were deposited on the back surface to ensure a uniform anodic current distribution.[9] The porous Si layers were formed by anodization in a HF solution at a constant current density of 30 mA/cm^2 for 20 min. The anodizing solution used was a 1:1 dilution of 49 wt % aqueous HF solution in ethyl alcohol. After rinsing in deionized water, chemical etching in a 1.5 wt % aqueous HF solution was carried out for 30 min.

The sample was prepared about one week before experiment, and the oxidation level is expected to be relatively low. The sample was mounted in a flow-type He cryostate in a He atmosphere and excited by a DCM dye laser. In time-resolved measurements, 10-μsec rectangular pulses with repetition rates of 160 or 20 Hz were produced from cw light by an acoustic-optic modulator and focused on to the sample by a cylindrical lens. The laser power at the peak of the pulse was restricted to 10 mW. The luminescence signal was analyzed by a 25-cm single-grating monochromator equipped with a photomultiplier (Hamamatsu R928), and then recorded and averaged by a digital oscilloscope with a total response time of 1 or 150 μsec depending on the load resister of the anode. The spectral response of the whole system was calibrated by using a tungsten standard lamp and the spectra were corrected for this response.

RESULTS

The luminescence spectrum at 5 K under excitation by 1.873-eV light is shown in the inset of Fig. 1. After sensitivity correction, a peak appears at 1.48 eV, which is lower than that under green light excitation. The decay curves were measured at 1.459 and 1.698 eV with a band pass of about 30 meV. The origin ($t=0$) of the time axis is taken at the trailing edge of the excitation pulse. As shown in Fig. 1, the lifetime is shorter and the decay curve is more nonexponential at higher photon energy. This tendency is in accordance with previous reports [feature (ii) above], and seen for all temperatures. Hereafter, we discuss mainly the behavior at 1.459 eV, which is near the maximum of the luminescence spectrum.

Figure 2 shows the decay curves at several temperatures. Although we cannot see a fast-decay component in our measurements if it exists, we can estimate the upper limit of the contribution of components faster than the pulse width. If there is a decay component much faster than the pulse width, it will exactly follow the rectangular pulse shape. Therefore, the time-integrated intensity of the fast component will not exceed the area of the observed luminescence signal during the excitation pulse. The contribution of this fast-decay component estimated in this way is less than 2% or 7% at 107 or 208 K, respectively, while at 271 K the upper limit is 25%. Therefore, we can consider that the main decay process is seen on our time scale at least below 208 K. The typical time constant of the decay changes drastically with temperature from several tens of μsec at RT to several msec at 5 K. In addition, the shape is very close to a single exponential around 40 K, but is strongly nonexponential at higher temperatures and slightly nonexponential at 5 K. From the time integration of the curves, we obtained the temperature dependence of luminescence intensity, which is shown in Fig. 3 by closed circles. The intensity increases by a factor of about 40 from RT to 80 K and then slightly decreases at lower temperatures.

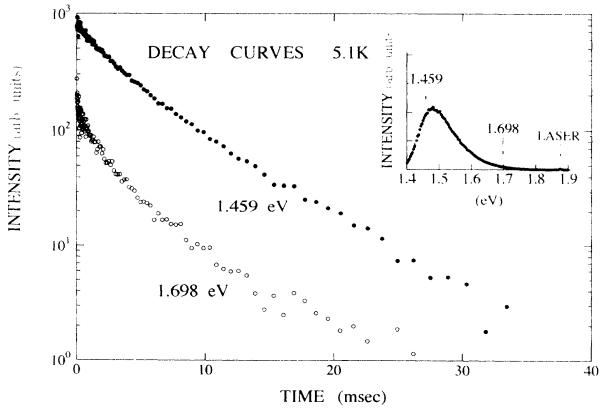

FIG. 1. Luminescence decay curves at 1.698 eV (7300 Å) (open circles) and 1.459 eV (8500 Å) (solid circles), measured at 5 K. The inset shows the spectrum at 5 K under excitation by 1.873-eV (6620 Å) laser light. The decay curves are taken at the positions indicated by arrows.

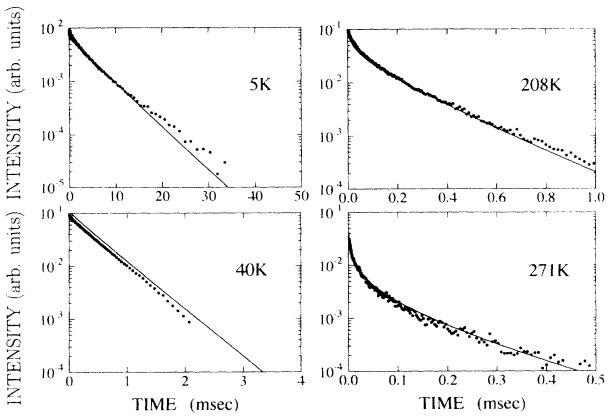

FIG. 2. Details of the decay profiles at 5, 40, 208, and 271 K, under excitation by 1.873-eV light and observed at 1.459 eV. The dots stand for the experimental data and the curves are the calculated results (see text).

DISCUSSION

As seen from Fig. 2, the decay curve at 40 K is very close to a single exponential, and, even near RT where the shape is nonexponential, the tail of the curve seems rather straight in the semilogarithmic plot. We try to un-

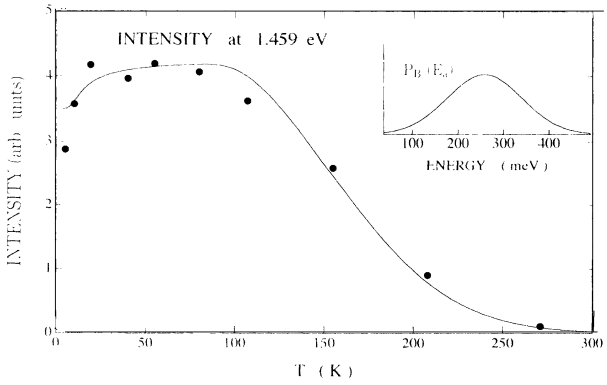

FIG. 3. Time-integrated intensity of the luminescence from experiment (closed circles) and calculation from a time integral of Eq. (8) (solid curve). The inset shows the Gaussian distribution given by Eq. (7) and used in the calculation.

derstand this part first. In interpreting the nonexponential decay in porous Si, some authors[2,8] have suggested a recombination of spatially separated carriers, which is known to occur in amorphous semiconductors.[10] In this case, however, the long tail should exist at any temperature and it is hard to understand the almost exponential decay at 40 K.

In the following, we introduce a phenomenological model based on radiative and nonradiative recombination of electron-hole pairs confined in microstructures of the Si. The morphology of the microstructures in porous Si has not yet been established. Although small crystalline areas of several tens of Å are often observed in electron microscope images, the three-dimensional shape or connectivity is not clear. For simplicity of modeling, we assume Si particles of the same shape, spheres for example. Other possibilities will be discussed later. Owing to the quantum-confinement effect, smaller particles have a larger band gap, which leads to shorter-wavelength luminescence. According to our previous investigation on a similar sample, the radiative recombination takes place mainly from the lowest exciton state.[11] Therefore, when we observe the luminescence at a fixed photon energy, the relevant Si particle size is the same, neglecting the phonon energy, which may be involved in the luminescence process. Even if the size is constant, we can still expect a distribution in the luminescence lifetimes. Thus we assume an inhomogeneous distribution in the lifetimes of the luminescence centers. Then the nonexponential profile of the decay curves can be interpreted as a superposition of exponentials with different time constants. In this picture, the slope at the tail of the decay curve reflects the lifetime of the particles which have the longest lifetime. The decay rate (reciprocal of the lifetime) determined from the slope of the tail is shown in Fig. 4 by closed circles as a function of $1/T$ (K^{-1}). As the temperature rises, the decay rate increases, following an activation-type temperature dependence from around 10 K (with an activation energy of 3.45 meV). This result is similar to that observed by 't Hooft *et al.*, although their activation energy[6] (13.5 meV) is quite different from ours. We interpret this temperature dependence as that of the radiative recombination rates.[6,7]

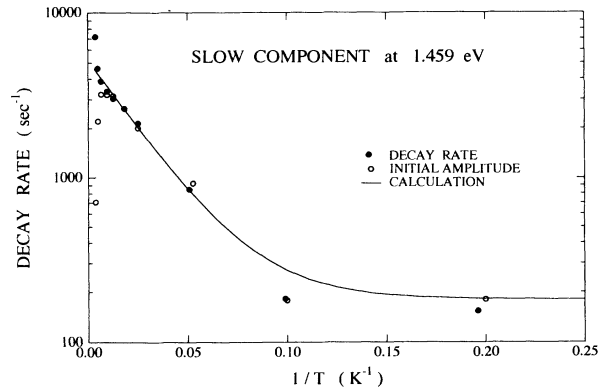

FIG. 4. Solid circles represent the temperature dependence of the decay rate determined at the tails of the decay curves plotted as a function of reciprocal temperature. The open circles stand for the initial amplitude of the luminescence signal; the ordinate scale is adjusted to fit the decay-rate curve. The curve is calculated from Eq. (2).

For a single Si particle, the luminescence intensity at the time t after a pulsed excitation will be given by

$$I(t)=I_0R_r\exp[-(R_r+R_n)t] , \tag{1}$$

if the pulse width and the detector response are much faster than $1/(R_r+R_n)$. Here, R_r and R_n are the radiative and nonradiative decay rates, respectively, and I_0 is a constant. As can be seen from this equation, $I(0)=I_0R_r$; that is, at the very beginning of the decay, the luminescence intensity should be proportional to the radiative decay rate, no matter whether a nonradiative process exists or not. This is true also for the total luminescence intensity from a group of luminescence centers with different R_n, so long as the value of R_r is common in this group. The open circles in Fig. 4 show the observed initial amplitude (at the trailing edge of the laser pulse) of the luminescence signal. Its behavior is quite parallel with that of the decay rate from 5 up to 155 K. The deviation at 208 and 271 K is ascribed to the finite excitation-pulse width and the slow response of the detection system. The good agreement suggests the validity of the above-mentioned interpretation that the time constant at the tail of the decay curve corresponds to the radiative decay rate R_r. Thus we can consider this curve as the temperature dependence of the radiative recombination rate, which is common to all the contributing luminescence centers observed at this photon energy, and is fitted by the equation

$$R_r=A_0\exp(-E_0/k_BT)+R_0 . \tag{2}$$

For the curve in Fig. 4 $A_0=5000\ \text{sec}^{-1}$, $E_0=3.45$ meV (40 K), and $R_0=180\ \text{sec}^{-1}$.

Next we consider the origin of the nonexponential decay. As the decay curve is very close to a single exponential at 40 K (Fig. 2), where the quantum efficiency is highest (Fig. 3), the radiative decay rate seems to have no large distribution. The nonexponential feature is more likely to be related to a distribution in the nonradiative decay rate. A nonradiative process is definitely necessary to interpret both the nonexponential shape and the significant luminescence quenching at higher temperatures. We suppose that there are quantum-confined electrons and holes in Si microstructures. Some of the excited carriers will recombine radiatively and others may escape from this limited region through the barrier and recombine nonradiatively. Although it is not apparent which carriers (electrons or holes) are important for such a process, we consider the behavior of the electron for simplicity. The nonradiative decay rate R_n is the sum of a tunneling process and a thermally activated process. First, we consider the tunneling process. The transmission probability of a particle through a rectangular potential barrier in one dimension is given by[12]

$$p=\left[1+\frac{V_0^2\sinh^2\beta a}{4E(V_0-E)}\right]^{-1} , \tag{3}$$

where

$$\beta a = E_a^{1/2}/\gamma \tag{4}$$

and

$$\gamma = (\hbar^2/2ma^2)^{1/2} . \tag{5}$$

Here, E is the kinetic energy of the carrier, $V_0 = E_a + E$ is the height of the potential barrier measured from the bottom of the bulk conduction band, and E_a is the barrier height measured from the lowest energy level of the confined carrier. Neglecting the confinement energy of the hole, E is equal to $E_L - E_g$, where E_L is the observed luminescence photon energy, and $E_g = 1.17$ eV is the indirect-band-gap energy of bulk Si.[13] m is the effective mass of the carrier, and a is the thickness of the barrier. Thus, in our experimental conditions, $E = 1.46 - 1.17 = 0.29$ eV and p can be evaluated for a given value of γ and E_a. The attempt frequency f_0 of this tunneling process is roughly estimated from the traverse time of the carrier in the lowest state in a Si particle of 30 Å in diameter. Assuming an effective mass of $m_t = 0.19m_0$ (in the X valley),[13] f_0 is estimated to be of the order of 10^{14} sec^{-1}.

Secondly, we add a thermally activated process, and the total nonradiative recombination rate becomes

$$R_n = f_0 p + f \exp(-E_a/k_B T) , \tag{6}$$

where f is the attempt frequency for the thermally activated process. Although we have no information about the distribution of the barrier height E_a, we used a Gaussian distribution centered at E_c,

$$P_B(E_a) = P_{B0} \exp\{-[(E_a - E_c)/w]^2\} . \tag{7}$$

The total luminescence intensity is then given by

$$I_{\text{tot}}(t) = \int_0^\infty P_B(E_a) I(t)\, dE_a = I_0 R_r \int_0^\infty P_B(E_a) \exp\{-[R_r + R_n(E_a)]t\}\, dE_a . \tag{8}$$

Here R_n is defined by Eq. (6) as a function of E_a.

We tried to find a set of the four parameters f, γ, E_c, and w that can fit simultaneously the shape of the ten decay curves obtained between 5 K and RT. The best set of parameters is found to be $f = 10^{12}$ sec^{-1}, $\gamma = 1.02$ $\text{meV}^{1/2}$, $E_c = 259$ meV (3000 K), and $w = 116$ meV (1350 K), but it is not clear whether this is the unique solution. The distribution function used is shown in the inset of Fig. 3. The decay curves *including the amplitude* can be calculated from Eq. (8) for arbitrary temperature; the results are shown in Fig. 5 together with some typical experimental data for various temperatures. The agreement seems almost perfect. The increase of the initial amplitude from 5 to 80 K corresponds to the increase of the radiative transition rate. With further increase of temperature, the mean lifetime decreases rapidly, mainly due to nonradiative decay. Therefore, the initial amplitude does not change much, and the decay curve becomes more and more nonexponential. The detailed shape is compared in Fig. 2. The exponential behavior around 40 K and the nonexponential shape above 200 K are well reproduced. Furthermore, the time-integrated intensity from this calculation shown in Fig. 3 (solid curve) is in good agreement with experiment. The decrease of intensity at higher temperature is ascribed to thermally activated nonradiative decay and the slight decrease at the lowest temperature is ascribed to tunneling escape, which is not very fast but cannot be ignored at low temperatures, because the radiative lifetime is extremely long at this temperature. The maximum quantum yield in this calculation is about 85% around 80 K. At this temperature, the radiative transition is already fast enough to overwhelm the tunneling escape owing to the small activation energy for the radiative process, and thermally activated escape is still not important due to the relatively large activation energy for the nonradiative process.

In this kind of fitting, the attempt frequency is difficult to determine in general. Actually, it is not impossible to get similar result with one or two orders of magnitude difference in the values for f, with a slight loss in fitting quality. One possibility is to assume $f = f_0$, that is, 10^{14} sec^{-1}, but his value is apparently an overestimation, because the equilibration between the lattice and electron systems which is necessary for thermal activation requires a time on the order of 10^{-13} sec in bulk semiconductors.[14] Therefore, the value of f used in the fitting is not unreasonable. Using Eq. (5), the barrier thickness is estimated to be 150 Å from $\gamma = 1.02$ and $m_t = 0.19m_0$ or 70 Å from $m_l = 0.9m_0$.

The mean barrier height 259 meV is one order of magnitude lower than the band offset between Si and SiO_2, which was assumed in the analysis by Vial *et al.*[5] We can consider two possible reasons for this. One possibility is that the barrier layer consists of material different from the simple oxide. Actually, the existence of Si-H_n and Si-OH has been verified from ir absorption spectroscopy in a sample made by the same procedure as our present sample.[9] These might have different band offsets. In this case, we have to assume that the band offset of the material behind the barrier is negative relative to the barrier material. This might be possible if the outside of the particle is surrounded by amorphous-Si-like material. The second possibility is a geometrical effect . If the particles

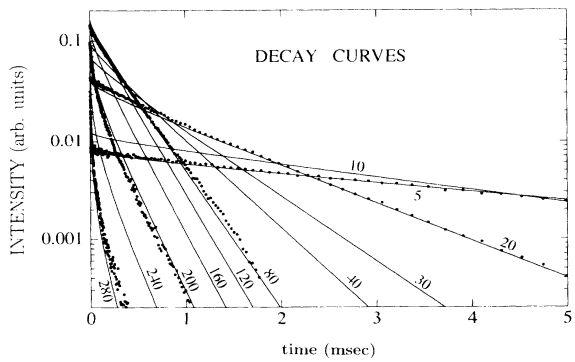

FIG. 5. Solid curves are the decay curves calculated by Eq. (8) at various temperatures, which are indicated by the numbers close to each curve. The dots are the typical experimental data taken at 5, 19, 80, 208, and 271 K.

of Si contact each other, the situation may be approximated by a rodlike shape with fluctuating diameter. The carrier will be trapped by two successive bottlenecks in a spatially limited region, where the diameter is relatively large. In this case each limited region will behave like a particle and the bottlenecks will act as low barriers with relatively large thickness. A carrier with sufficient energy will travel around the whole volume of the connected particles, and the probability of nonradiative decay will increase drastically.

As for the thermal activation process in the radiative decay rate [E_0 in Eq. (2)], 't Hooft *et al.*[6] considered a phonon-assisted process with a phonon energy of 13.5 meV. However, it has been shown that the energy of phonons involved in the transition is far larger (61 meV) and no-phonon transitions have a contribution of the same order of magnitude.[11] Furthermore, in our case the value of 3.45 meV (28 cm^{-1}) for the activation energy is very different from the value cited above, and the phonon density of states in this region will be very low. Therefore it is hard to ascribe the activation energy to a phonon energy. One possible candidate for the activation energy is the singlet-triplet splitting of the confined exciton.[7] The close resemblance of our temperature dependence of the radiative lifetime to that in Fig. 2(b) of Ref. 7 supports this interpretation. However, the value of the activation energy is 13 meV at 1.77 eV in Ref. 7 and is substantially larger than our value. The difference might be ascribed to the difference in the particle size, corresponding to the observed photon energy, or the morphology of the microscopic structures. Thermally activated migration of carriers might be responsible, but the situation is not clear at present.

Based on this model, the decay behavior in earlier stages can be calculated. With the same parameters used in the above calculation, the nsec and psec components appear as shown in Fig. 6 at 300 K. Although the sample preparation procedures and experimental conditions may be different, the profile qualitatively reproduces the data reported by Matsumoto *et al.*[2] Thus, the feature (iv) defined in the Introduction can be understood on all time scales, and the psec components are conjectured to be caused by a fast nonradiative process. The initial redshift of the luminescence in the psec range can also be understood in our model, combined with the explanation of feature (ii) discussed below. Assuming larger barrier heights, we can reproduce the single-exponential decays and constant quantum yield reported by 't Hooft *et al.*[6]

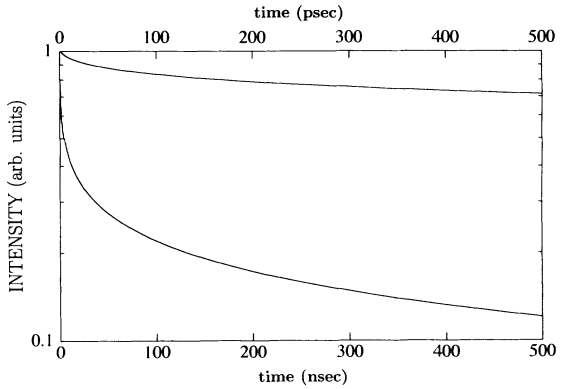

FIG. 6. Calculated decay curves in the psec (upper curve) and nsec ranges (lower curve) at 300 K. Note the different scale of the time axes.

The feature (ii) is in accordance with our model, because luminescence at higher photon energy corresponds to larger confinement energy and the effective barrier height will be reduced, which results in faster nonradiative decay. The tendency to increasing nonexponential character at higher phonon energy, as seen in Fig. 1, can also be understood in this way.

The conclusions derived from our model are summarized as follows: (a) A radiative process is reflected in the tail and the initial amplitude of the decay curve. (b) The nonexponential decay and large temperature dependence of the luminescence intensity are indications of nonradiative decay. Further experimental investigation on various time scales on samples with different preparation methods, especially with various oxidation levels, is desirable to check the validity of this model.

ACKNOWLEDGMENTS

A.N. would like to thank Dr. T. Ito, T. Itakura, and N. Nakayama for their encouragement.

[1]L. T. Canham, Appl. Phys. Lett. **57**, 1046 (1990).
[2]T. Matsumoto, M. Daimon, T. Futagi, and H. Mimura, Jpn. J. Appl. Phys. **31**, L619 (1992); T. Matsumoto, T. Futagi, H. Mimura, and Y. Kanemitsu, Phys. Rev. B **47**, 13 876 (1993).
[3]S. Gardelis, J. S. Rimmer, P. Dawson, B. Hamilton, R. A. Kubiak, T. E. Whall, and E. H. C. Parker, Appl. Phys. Lett. **59**, 2118 (1991).
[4]T. Miyoshi, Kyu-Seok Lee, and Y. Aoyagi, Jpn. J. Appl. Phys. **31**, 2470 (1992).
[5]J. C. Vial, A. Bsiesy, F. Gaspard, R. Hérino, M. Ligeon, F. Muller, R. Romestain, and R. M. Macfarane, Phys. Rev. B **45**, 14 171 (1992).
[6]G. W. 't Hooft, Y. A. R. R. Kessener, G. L. J. A. Rikken, and A. H. J. Venhuizen, Appl. Phys. Lett. **61**, 2344 (1992).
[7]P. D. J. Calcott, K. J. Nash, L. T. Canham, M. J. Kane, and D. Brumhead, J. Phys. Condens. Matter **5**, L91 (1993).
[8]N. Ookubo, H. Ono, Y. Ochiai, Y. Mochizuki, and S. Matsui, Appl. Phys. Lett. **61**, 940 (1992).
[9]A. Nakajima, I. Itakura, S. Watanabe, and N. Nakayama, Appl. Phys. Lett. **61**, 46 (1992).
[10]C. Tsang and R. A. Street, Phys. Rev. B **19**, 3027 (1979).
[11]T. Suemoto, K. Tanaka, A. Nakajima, and T. Itakura, Phys. Rev. Lett. **70**, 3659 (1993).
[12]See, for example, L. I. Schiff, *Quantum Mechanics*, 3rd ed. (McGraw-Hill, New York, 1955).
[13]*Landolt-Börnstein Tables*, edited by O. Madelung, M. Schulz, and H. Weiss, New Series, Vol. 17 (Springer-Verlag, Berlin, 1982).
[14]J. A. Kash, J. C. Tsang, and J. M. Hvam, Phys. Rev. Lett. **54**, 2151 (1985).